Ain Shams Engineering Journal 16 (2025) 103522

Contents lists available at ScienceDirect

Ain Shams Engineering Journal

journal homepage: https://www.sciencedirect.com

Full Length Article

Mechanical modeling of complex $\mathcal{NLS}$ shock optimistic waves with Schrödinger frame

Fatih Şevgin [a,*], Talat Körpinar [b], Ali Akgül [c,d,e,f], Qasem Al-Mdallal [g]

[a] Muş Alparslan University, Department of Construction Technology, 49250, Muş, Turkey
[b] Muş Alparslan University, Department of Mathematics, 49250, Muş, Turkey
[c] Department of Electronics and Communication Engineering, Saveetha School of Engineering, SIMATS, Chennai, Tamilnadu, India
[d] Siirt University, Art and Science Faculty, Department of Mathematics, 56100 Siirt, Turkey
[e] Department of Computer Engineering, Biruni University, 34010 Topkapı, Istanbul, Turkey
[f] Near East University, Mathematics Research Center, Department of Mathematics, Near East Boulevard, PC: 99138, Nicosia /Mersin 10 – Turkey
[g] Department of Mathematical Sciences, P.O. Box 17551, UAE University, Al-Ain, United Arab Emirates

ARTICLE INFO

Keywords:
Dam-break model
Schrödinger model
Shallow wave energy
Turbulence model

ABSTRACT

In this article, we describe antiferromagnetic Heisenberg super-fluid complex dispersive $\mathcal{NLS}$ shock electromotive wave for $\phi(\chi_1), \phi(\chi_2), \phi(\chi_3)$tension dam-break antiferromagnetic microfluidics with non-linear hermitian Schrödinger model. Then, we construct Lorentzian antiferromagnetic dispersive complex $\mathcal{NLS}$ Heisenberg shock optimistic waves for $\phi(\chi_1), \phi(\chi_2), \phi(\chi_3)$ dam-break antiferromagnetic intensity in Lorentzian hermitian space. Thus, we have antiferromagnetic Heisenberg hermitian complex $\mathcal{NLS}$ electromotive tension microscales. Finally, we illustrate Schrödinger antiferromagnetic thermocomplex solid magnetic $\mathcal{NLS}$ pressure of $\phi(\chi_1), \phi(\chi_2), \phi(\chi_3)$ tension antiferromagnetic wave energy in Lorentzian hermitian space associated with Heisenberg complex dam-break potential in shallow water.

1. Introduction

The modeling of wave energy and its applications into usable forms has garnered significant attention in dam break theory with renewable energy systems. Shallow wave energy has been constructed by tension fluid and shallow water environments for wave energy harnessing. The transformation of wave energy from deep water to nearshore regions involves complex interactions influenced by factors such as wave directionality, water depth, and local tidal conditions. These factors not only affect the gross wave energy resource but also determine the exploitable wave energy, which is a more accurate measure of the potential for energy extraction [1–5].

In shallow water systems, the dynamics of wave energy conversion are complicated by the interaction of waves with the seabed and the presence of oscillating bodies or wave energy converters (WECs). Physical experimental studies have demonstrated that shallow oscillating systems, such as heaving floats coupled with surging paddles, can significantly enhance energy capture in shallow water compared to single-body systems [6–24].

The modeling of wave energy systems in shallow water also requires high-resolution assessments that account for local tidal and wind influences. Advanced wave modeling systems have been described to evaluate wave energy resources in coastal areas, providing valuable insights into the spatial and temporal variability of wave energy [25–31].

In parallel with advancements in wave energy research, there has been growing interest in the application of nonlinear Schrödinger (NLS) models to describe complex wave phenomena. These models, which are rooted in quantum mechanics, have been extended to describe a wide range of physical systems, including optical solitons, fluid dynamics, and magnetic materials. For instance, the antiferromagnetic Schrödinger model has been used to characterize nonlinear electromotive waves in microscale systems, providing a framework for understanding the behavior of complex dispersive waves in magnetic and fluidic environments. Similarly, the binormal Schrödinger system has been applied to study light diffusion in curved paths, offering new insights into the geometric and optical properties of wave propagation [32–39].

* Corresponding author.
E-mail addresses: f.sevgin@alparslan.edu.tr (F. Şevgin), aliakgul00727@gmail.com (A. Akgül), q.almdallal@uaeu.ac.ae (Q. Al-Mdallal).

https://doi.org/10.1016/j.asej.2025.103522
Received 31 October 2024; Received in revised form 12 April 2025; Accepted 17 May 2025
Available online 10 June 2025

Nomenclature

χ_1, χ_2, χ_3	electromagnetic wave fields	$\mathcal{B}^{nls}$	magnetic wave field
∇	covariant derivative	$\times_{\mathcal{L}}$	Lorentzian product
ϕ	Lorentz force	$\varkappa$	dam-break potential
σ	quasi-slope potential	Δ^{nls}	tension dam-break microfluidics

This article presents a mechanical modeling framework for complex NLS shock optimistic waves within a Schrödinger model. We focus on the antiferromagnetic Heisenberg super-fluid complex dispersive NLS shock electromotive waves, which are characterized by tension dam-break dynamics in microscale antiferromagnetic systems. By constructing Lorentzian antiferromagnetic dispersive complex NLS Heisenberg shock optimistic waves, we aim to elucidate the interplay between wave energy, magnetic intensity, and fluid dynamics in shallow water environments. Our approach integrates concepts from nonlinear hermitian Schrödinger models and Lorentzian geometry, providing a comprehensive understanding of the microscale phenomena associated with wave energy conversion [40–49].

This work is motivated by the need to bridge the gap between theoretical models and practical applications in wave energy modeling. By leveraging insights from recent studies on wave energy resources, oscillating body systems, and nonlinear Schrödinger models, we aim to develop a robust framework for modeling complex wave phenomena in shallow water. The results of this study have the potential to inform the design of next-generation WECs and to enhance our understanding of the fundamental principles governing wave energy conversion in complex environments.

Aim of our work, a general development method is recommended for antiferromagnetic Heisenberg super-fluid complex dispersive $\mathcal{NLS}$ shock model with illustrations of results in Lorentzian hermitian space. We consider that the cases of Lorentzian antiferromagnetic dispersive complex $\mathcal{NLS}$ Heisenberg shock optimistic waves for Lorentz forces. The advantage of our used technique on other methods: we couple both theory of complex geometry of particles and antiferromagnetic theory, we design to recover a special class of fractional flow equations. The engineering applications of these models are magnetic dam-break surfaces.

The paper is organized as follows. First, we construct antiferromagnetic Heisenberg super-fluid complex dispersive $\mathcal{NLS}$ shock electromotive wave for $\phi(\chi_1), \phi(\chi_2), \phi(\chi_3)$ tension dam-break antiferromagnetic microfluidics with non-linear hermitian Schrödinger model. Then, we construct Lorentzian antiferromagnetic dispersive complex $\mathcal{NLS}$ Heisenberg shock optimistic waves for $\phi(\chi_1), \phi(\chi_2), \phi(\chi_3)$ dam-break antiferromagnetic intensity in Lorentzian hermitian space. Thus, we have antiferromagnetic Heisenberg hermitian complex $\mathcal{NLS}$ electromotive tension microscales. Finally, we illustrate Schrödinger antiferromagnetic thermocomplex solid magnetic $\mathcal{NLS}$ pressure of $\phi(\chi_1), \phi(\chi_2), \phi(\chi_3)$ tension antiferromagnetic wave energy in Lorentzian hermitian space associated with Heisenberg complex dam-break potential in shallow water.

2. NLS model

Non-linear Schrödinger system is

$$\chi_1 = \mathbf{t},\ \chi_2 = \frac{\mathbf{f}_2 + i\mathbf{f}_1}{\sqrt{2}},\ \chi_3 = \frac{\mathbf{f}_2 - i\mathbf{f}_1}{\sqrt{2}},$$

where

$$0 = \langle \chi_1, \chi_2 \rangle_{\mathcal{L}} = \langle \chi_1, \chi_3 \rangle_{\mathcal{L}} = \langle \chi_2, \chi_2 \rangle_{\mathcal{L}} = \langle \chi_3, \chi_3 \rangle_{\mathcal{L}}$$
$$-1 = \langle \chi_1, \chi_1 \rangle_{\mathcal{L}},\ 1 = \langle \chi_2, \chi_3 \rangle_{\mathcal{L}},$$

and

$$\chi_1 \times_{\mathcal{L}} \chi_2 = i\chi_2,\ \chi_3 \times_{\mathcal{L}} \chi_1 = i\chi_3,\ \chi_2 \times_{\mathcal{L}} \chi_3 = -i\chi_1.$$

Then

$$\nabla_s \chi_1 = \mathcal{F}\chi_2 + \mathcal{F}^*\chi_3,$$
$$\nabla_s \chi_2 = \mathcal{F}^*\chi_1,$$
$$\nabla_s \chi_3 = \mathcal{F}\chi_1,$$

and

$$\nabla_v \chi_1 = i\mathcal{F}_s\chi_2 - i\mathcal{F}_s^*\chi_3,$$
$$\nabla_v \chi_2 = -i\mathcal{F}_s\chi_1 + i\mathcal{F}\mathcal{F}^*\chi_2,$$
$$\nabla_v \chi_3 = i\mathcal{F}_s\chi_1 - i\mathcal{F}\mathcal{F}^*\chi_3,$$

where

$$\mathcal{F} = \frac{1}{\sqrt{2}}(\mu_2 - i\mu_1), \mathcal{F}^* = \frac{1}{\sqrt{2}}(\mu_2 + i\mu_1).$$

Heisenberg Lorentz forces and magnetic field are given by

$$\phi(\chi_1) = \left(\frac{\mathcal{F}}{\sqrt{2}}\cosh\varphi + \frac{\mathcal{F}^*}{\sqrt{2}}\cosh\varphi\right)\mathbf{e}_1 + \left(\frac{\mathcal{F}}{\sqrt{2}}(\varphi\mathcal{L} + i\mathcal{L}^*)\right.$$

$$+\frac{\mathcal{F}^*}{\sqrt{2}}(\varphi\mathcal{L}-i\mathcal{L}^*))\mathbf{e}_2+(\frac{\mathcal{F}}{\sqrt{2}}(\varphi\mathcal{L}^*+i\mathcal{L})+\frac{\mathcal{F}^*}{\sqrt{2}}(\varphi\mathcal{L}^*-i\mathcal{L}))\mathbf{e}_3$$

$$\phi(\chi_2)=(\mathcal{F}^*\varphi+\frac{\sigma}{\sqrt{2}}\cosh\varphi)\mathbf{e}_1+(\cosh\varphi\mathcal{L}\mathcal{F}^*+\frac{\sigma}{\sqrt{2}}(\varphi\mathcal{L}+i\mathcal{L}^*))\mathbf{e}_2$$

$$+(\frac{\sigma}{\sqrt{2}}(\varphi\mathcal{L}^*+i\mathcal{L})+\mathcal{F}^*\cosh\varphi\mathcal{L}^*)\mathbf{e}_3$$

$$\phi(\chi_3)=(-\frac{\sigma}{\sqrt{2}}\cosh\varphi+\mathcal{F}\varphi)\mathbf{e}_1+(\cosh\varphi\mathcal{F}\mathcal{L}-\frac{\sigma}{\sqrt{2}}(\varphi\mathcal{L}-i\mathcal{L}^*))\mathbf{e}_2$$

$$+(-\frac{\sigma}{\sqrt{2}}(\varphi\mathcal{L}^*-i\mathcal{L})+\cosh\varphi\mathcal{L}^*\mathcal{F})\mathbf{e}_3$$

$$\mathcal{B}^{nls}=(\frac{i\mathcal{F}}{\sqrt{2}}\cosh\varphi-i\varphi\sigma-\frac{i\mathcal{F}^*}{\sqrt{2}}\cosh\varphi)\mathbf{e}_1+(\frac{i\mathcal{F}}{\sqrt{2}}(\varphi\mathcal{L}+i\mathcal{L}^*)-\frac{i\mathcal{F}^*}{\sqrt{2}}(\varphi\mathcal{L}-i\mathcal{L}^*)$$

$$-i\cosh\varphi\sigma\mathcal{L})\mathbf{e}_2+(-i\sigma\cosh\varphi\mathcal{L}^*+\frac{i\mathcal{F}}{\sqrt{2}}(\varphi\mathcal{L}^*+i\mathcal{L})-\frac{i\mathcal{F}^*}{\sqrt{2}}(\varphi\mathcal{L}^*-i\mathcal{L}))\mathbf{e}_3$$

where σ is a differentiable quasi-slope potential.

It can be seen that

$$\nabla_s\phi(\chi_1)=2\mathcal{F}\mathcal{F}^*\chi_1+\mathcal{F}_s\chi_2+\mathcal{F}_s^*\chi_3,$$

$$\nabla_s\phi(\chi_2)=(\mathcal{F}_s^*+\sigma\mathcal{F}^*)\chi_1+(\sigma_s+\mathcal{F}^*\mathcal{F})\chi_2+(\mathcal{F}^*)^2\chi_3,$$

$$\nabla_s\phi(\chi_3)=(\mathcal{F}_s-\sigma\mathcal{F})\chi_1+(\mathcal{F})^2\chi_2+(\mathcal{F}^*\mathcal{F}-\sigma_s)\chi_3,$$

$$\nabla_s\mathcal{B}^{nls}=-i\sigma_s\chi_1+i(\mathcal{F}_s-\sigma\mathcal{F})\chi_2-i(\mathcal{F}_s^*+\sigma\mathcal{F}^*)\chi_3.$$

3. Heisenberg super-fluid complex magnetic $\phi(\chi_1)$ dam-break antiferromagnetic microfluidics

First, we have

$$\nabla_v\phi(\chi_1)=(i(\mathcal{F}^*\mathcal{F}_s-\mathcal{F}_s\mathcal{F})\varphi+\frac{1}{\sqrt{2}}\cosh\varphi(\mathcal{F}_v+i\mathcal{F}^2\mathcal{F}^*)+\frac{1}{\sqrt{2}}(\mathcal{F}_v^*$$

$$-i\mathcal{F}(\mathcal{F}^*)^2)\cosh\varphi)\mathbf{e}_1+(\frac{1}{\sqrt{2}}(\mathcal{F}_v+i\mathcal{F}^2\mathcal{F}^*)(\varphi\mathcal{L}+i\mathcal{L}^*)+i\cosh\varphi\mathcal{L}(\mathcal{F}^*\mathcal{F}_s$$

$$-\mathcal{F}_s\mathcal{F})+\frac{1}{\sqrt{2}}(\varphi\mathcal{L}-i\mathcal{L}^*)(\mathcal{F}_v^*-i\mathcal{F}(\mathcal{F}^*)^2))\mathbf{e}_2+(i\cosh\varphi\mathcal{L}^*(\mathcal{F}^*\mathcal{F}_s-\mathcal{F}_s\mathcal{F})$$

$$+\frac{1}{\sqrt{2}}(\varphi\mathcal{L}^*+i\mathcal{L})(\mathcal{F}_v+i\mathcal{F}^2\mathcal{F}^*)+\frac{1}{\sqrt{2}}(\mathcal{F}_v^*-i\mathcal{F}(\mathcal{F}^*)^2)(\varphi\mathcal{L}^*-i\mathcal{L}))\mathbf{e}_3.$$

⋈ *Heisenberg super-fluid complex dispersive $\mathcal{NLS}$ shock electromotive wave for $\phi(\chi_1)$ tension dam-break microfluidics is*

$$\Delta^{nls}\phi(\chi_1)=-\frac{d}{dv}\int_{\Phi}(-(i\cosh\varphi\mathcal{L}^*(\mathcal{F}^*\mathcal{F}_s-\mathcal{F}_s\mathcal{F})+\frac{1}{\sqrt{2}}(\varphi\mathcal{L}^*+i\mathcal{L})(\mathcal{F}_v+i\mathcal{F}^2\mathcal{F}^*)$$

$$+\frac{1}{\sqrt{2}}(\mathcal{F}_v^*-i\mathcal{F}(\mathcal{F}^*)^2)(\varphi\mathcal{L}^*-i\mathcal{L}))(-i\sigma\cosh\varphi\mathcal{L}^*+\frac{i\mathcal{F}}{\sqrt{2}}(\varphi\mathcal{L}^*+i\mathcal{L})-\frac{i\mathcal{F}^*}{\sqrt{2}}(\varphi\mathcal{L}^*-i\mathcal{L}))$$

$$+(\frac{i\mathcal{F}}{\sqrt{2}}\cosh\varphi-i\varphi\sigma-\frac{i\mathcal{F}^*}{\sqrt{2}}\cosh\varphi)(i(\mathcal{F}^*\mathcal{F}_s-\mathcal{F}_s\mathcal{F})\varphi+\frac{1}{\sqrt{2}}\cosh\varphi(\mathcal{F}_v+i\mathcal{F}^2\mathcal{F}^*)+\frac{1}{\sqrt{2}}(\mathcal{F}_v^*$$

$$-i\mathcal{F}(\mathcal{F}^*)^2)\cosh\varphi)+(\frac{i\mathcal{F}}{\sqrt{2}}(\varphi\mathcal{L}+i\mathcal{L}^*)-\frac{i\mathcal{F}^*}{\sqrt{2}}(\varphi\mathcal{L}-i\mathcal{L}^*)-i\cosh\varphi\sigma\mathcal{L})(\frac{1}{\sqrt{2}}(\mathcal{F}_v$$

$$+i\mathcal{F}^2\mathcal{F}^*)(\varphi\mathcal{L}+i\mathcal{L}^*)+i\cosh\varphi\mathcal{L}(\mathcal{F}^*\mathcal{F}_s-\mathcal{F}_s\mathcal{F})+\frac{1}{\sqrt{2}}(\varphi\mathcal{L}-i\mathcal{L}^*)(\mathcal{F}_v^*-i\mathcal{F}(\mathcal{F}^*)^2)))d\Phi.$$

⋈ *Lorentzian dispersive complex $\mathcal{NLS}$ Heisenberg shock optimistic waves for $\phi(\chi_1)$ dam-break intensity is*

$$\mathcal{F}^{nls}\phi(\chi_1)=(\frac{i\mathcal{F}}{\sqrt{2}}\cosh\varphi-i\varphi\sigma-\frac{i\mathcal{F}^*}{\sqrt{2}}\cosh\varphi)(i(\mathcal{F}^*\mathcal{F}_s-\mathcal{F}_s\mathcal{F})\varphi+\frac{1}{\sqrt{2}}\cosh\varphi(\mathcal{F}_v+i\mathcal{F}^2\mathcal{F}^*)$$

$$+\frac{1}{\sqrt{2}}(\mathcal{F}_v^*-i\mathcal{F}(\mathcal{F}^*)^2)\cosh\varphi)+(\frac{i\mathcal{F}}{\sqrt{2}}(\varphi\mathcal{L}+i\mathcal{L}^*)-\frac{i\mathcal{F}^*}{\sqrt{2}}(\varphi\mathcal{L}-i\mathcal{L}^*)$$

$$-i\cosh\varphi\sigma\mathcal{L})(\frac{1}{\sqrt{2}}(\mathcal{F}_v+i\mathcal{F}^2\mathcal{F}^*)(\varphi\mathcal{L}+i\mathcal{L}^*)+i\cosh\varphi\mathcal{L}(\mathcal{F}^*\mathcal{F}_s-\mathcal{F}_s\mathcal{F})+\frac{1}{\sqrt{2}}(\varphi\mathcal{L}$$

$$-i\mathcal{L}^*)(\mathcal{F}_v^*-i\mathcal{F}(\mathcal{F}^*)^2))-(i\cosh\varphi\mathcal{L}^*(\mathcal{F}^*\mathcal{F}_s-\mathcal{F}_s\mathcal{F})+\frac{1}{\sqrt{2}}(\varphi\mathcal{L}^*+i\mathcal{L})(\mathcal{F}_v+i\mathcal{F}^2\mathcal{F}^*)$$

$$+\frac{1}{\sqrt{2}}(\mathcal{F}_{\nu}^{*}-i\mathcal{F}(\mathcal{F}^{*})^{2})(\varphi\mathcal{L}^{*}-i\mathcal{L}))(-i\sigma\cosh\varphi\mathcal{L}^{*}+\frac{i\mathcal{F}}{\sqrt{2}}(\varphi\mathcal{L}^{*}+i\mathcal{L})-\frac{i\mathcal{F}^{*}}{\sqrt{2}}(\varphi\mathcal{L}^{*}-i\mathcal{L})).$$

⋈ *Schrödinger thermocomplex solid magnetic $\mathcal{NLS}$ pressure of $\phi(\chi_1)$ tension wave energy is*

$$\Upsilon^{nls}\phi(\chi_1)=\varkappa\int_{\Phi}((\frac{i\mathcal{F}}{\sqrt{2}}(\varphi\mathcal{L}+i\mathcal{L}^{*})-\frac{i\mathcal{F}^{*}}{\sqrt{2}}(\varphi\mathcal{L}-i\mathcal{L}^{*})-i\cosh\varphi\sigma\mathcal{L})(\frac{1}{\sqrt{2}}(\mathcal{F}_{\nu}$$

$$+i\mathcal{F}^{2}\mathcal{F}^{*})(\varphi\mathcal{L}+i\mathcal{L}^{*})+i\cosh\varphi\mathcal{L}(\mathcal{F}^{*}\mathcal{F}_{s}-\mathcal{F}_{s}\mathcal{F})+\frac{1}{\sqrt{2}}(\varphi\mathcal{L}-i\mathcal{L}^{*})(\mathcal{F}_{\nu}^{*}-i\mathcal{F}(\mathcal{F}^{*})^{2}))$$

$$-(i\cosh\varphi\mathcal{L}^{*}(\mathcal{F}^{*}\mathcal{F}_{s}-\mathcal{F}_{s}\mathcal{F})+\frac{1}{\sqrt{2}}(\varphi\mathcal{L}^{*}+i\mathcal{L})(\mathcal{F}_{\nu}+i\mathcal{F}^{2}\mathcal{F}^{*})+\frac{1}{\sqrt{2}}(\mathcal{F}_{\nu}^{*}-i\mathcal{F}(\mathcal{F}^{*})^{2})(\varphi\mathcal{L}^{*}$$

$$-i\mathcal{L}))(-i\sigma\cosh\varphi\mathcal{L}^{*}+\frac{i\mathcal{F}}{\sqrt{2}}(\varphi\mathcal{L}^{*}+i\mathcal{L})-\frac{i\mathcal{F}^{*}}{\sqrt{2}}(\varphi\mathcal{L}^{*}-i\mathcal{L}))+(\frac{i\mathcal{F}}{\sqrt{2}}\cosh\varphi-i\varphi\sigma$$

$$-\frac{i\mathcal{F}^{*}}{\sqrt{2}}\cosh\varphi)(i(\mathcal{F}^{*}\mathcal{F}_{s}-\mathcal{F}_{s}\mathcal{F})\varphi+\frac{1}{\sqrt{2}}\cosh\varphi(\mathcal{F}_{\nu}+i\mathcal{F}^{2}\mathcal{F}^{*})+\frac{1}{\sqrt{2}}(\mathcal{F}_{\nu}^{*}-i\mathcal{F}(\mathcal{F}^{*})^{2})\cosh\varphi))d\Phi,$$

where $\varkappa$ is Heisenberg complex dam-break potential in shallow water.

On the other hand, antiferromagnetic condition is

$$\phi(\chi_1)\times\nabla_{s}\phi(\chi_1)=(i(\mathcal{F}^{*}\mathcal{F}_{s}-\mathcal{F}\mathcal{F}_{s}^{*})\varphi+\frac{2}{\sqrt{2}}i(\mathcal{F}^{*})^{2}\cosh\varphi\mathcal{F}-\frac{2}{\sqrt{2}}i\mathcal{F}^{2}\mathcal{F}^{*}\cosh\varphi)\mathbf{e}_1$$

$$+(-\frac{2}{\sqrt{2}}i\mathcal{F}^{2}\mathcal{F}^{*}(\varphi\mathcal{L}+i\mathcal{L}^{*})+i\cosh\varphi(\mathcal{F}^{*}\mathcal{F}_{s}-\mathcal{F}\mathcal{F}_{s}^{*})\mathcal{L}+\frac{2}{\sqrt{2}}i(\mathcal{F}^{*})^{2}\mathcal{F}(\varphi\mathcal{L}-i\mathcal{L}^{*}))\mathbf{e}_2$$

$$+(i\cosh\varphi(\mathcal{F}^{*}\mathcal{F}_{s}-\mathcal{F}\mathcal{F}_{s}^{*})\mathcal{L}^{*}-\frac{2}{\sqrt{2}}i\mathcal{F}^{2}\mathcal{F}^{*}(\varphi\mathcal{L}^{*}+i\mathcal{L})+\frac{2}{\sqrt{2}}i(\mathcal{F}^{*})^{2}(\varphi\mathcal{L}^{*}-i\mathcal{L})\mathcal{F})\mathbf{e}_3.$$

⋈ *Antiferromagnetic Heisenberg super-fluid complex dispersive $\mathcal{NLS}$ shock electromotive wave for $\phi(\chi_1)$ tension dam-break antiferromagnetic microfluidics is*

$$\Delta_{afr}^{nls}\phi(\chi_1)=-\frac{d}{d\upsilon}\int_{\Phi}((-\frac{2}{\sqrt{2}}i\mathcal{F}^{2}\mathcal{F}^{*}(\varphi\mathcal{L}+i\mathcal{L}^{*})+i\cosh\varphi(\mathcal{F}^{*}\mathcal{F}_{s}-\mathcal{F}\mathcal{F}_{s}^{*})\mathcal{L}$$

$$+\frac{2}{\sqrt{2}}i(\mathcal{F}^{*})^{2}\mathcal{F}(\varphi\mathcal{L}-i\mathcal{L}^{*}))(\frac{i\mathcal{F}}{\sqrt{2}}(\varphi\mathcal{L}+i\mathcal{L}^{*})-\frac{i\mathcal{F}^{*}}{\sqrt{2}}(\varphi\mathcal{L}-i\mathcal{L}^{*})-i\cosh\varphi\sigma\mathcal{L})$$

$$+(i(\mathcal{F}^{*}\mathcal{F}_{s}-\mathcal{F}\mathcal{F}_{s}^{*})\varphi+\frac{2}{\sqrt{2}}i(\mathcal{F}^{*})^{2}\cosh\varphi\mathcal{F}-\frac{2}{\sqrt{2}}i\mathcal{F}^{2}\mathcal{F}^{*}\cosh\varphi)(\frac{i\mathcal{F}}{\sqrt{2}}\cosh\varphi-i\varphi\sigma$$

$$-\frac{i\mathcal{F}^{*}}{\sqrt{2}}\cosh\varphi)-(i\cosh\varphi(\mathcal{F}^{*}\mathcal{F}_{s}-\mathcal{F}\mathcal{F}_{s}^{*})\mathcal{L}^{*}-\frac{2}{\sqrt{2}}i\mathcal{F}^{2}\mathcal{F}^{*}(\varphi\mathcal{L}^{*}+i\mathcal{L})+\frac{2}{\sqrt{2}}i(\mathcal{F}^{*})^{2}(\varphi\mathcal{L}^{*}$$

$$-i\mathcal{L})\mathcal{F})(-i\sigma\cosh\varphi\mathcal{L}^{*}+\frac{i\mathcal{F}}{\sqrt{2}}(\varphi\mathcal{L}^{*}+i\mathcal{L})-\frac{i\mathcal{F}^{*}}{\sqrt{2}}(\varphi\mathcal{L}^{*}-i\mathcal{L})))d\Phi.$$

⋈ *Lorentzian antiferromagnetic dispersive complex $\mathcal{NLS}$ Heisenberg shock optimistic waves for $\phi(\chi_1)$ dam-break antiferromagnetic intensity is*

$$\mathcal{F}_{afr}^{nls}\phi(\chi_1)=-(i\cosh\varphi(\mathcal{F}^{*}\mathcal{F}_{s}-\mathcal{F}\mathcal{F}_{s}^{*})\mathcal{L}^{*}-\frac{2}{\sqrt{2}}i\mathcal{F}^{2}\mathcal{F}^{*}(\varphi\mathcal{L}^{*}+i\mathcal{L})$$

$$+\frac{2}{\sqrt{2}}i(\mathcal{F}^{*})^{2}(\varphi\mathcal{L}^{*}-i\mathcal{L})\mathcal{F})(-i\sigma\cosh\varphi\mathcal{L}^{*}+\frac{i\mathcal{F}}{\sqrt{2}}(\varphi\mathcal{L}^{*}+i\mathcal{L})-\frac{i\mathcal{F}^{*}}{\sqrt{2}}(\varphi\mathcal{L}^{*}$$

$$-i\mathcal{L}))+(-\frac{2}{\sqrt{2}}i\mathcal{F}^{2}\mathcal{F}^{*}(\varphi\mathcal{L}+i\mathcal{L}^{*})+i\cosh\varphi(\mathcal{F}^{*}\mathcal{F}_{s}-\mathcal{F}\mathcal{F}_{s}^{*})\mathcal{L}$$

$$+\frac{2}{\sqrt{2}}i(\mathcal{F}^{*})^{2}\mathcal{F}(\varphi\mathcal{L}-i\mathcal{L}^{*}))(\frac{i\mathcal{F}}{\sqrt{2}}(\varphi\mathcal{L}+i\mathcal{L}^{*})-\frac{i\mathcal{F}^{*}}{\sqrt{2}}(\varphi\mathcal{L}-i\mathcal{L}^{*})$$

$$-i\cosh\varphi\sigma\mathcal{L})+(i(\mathcal{F}^{*}\mathcal{F}_{s}-\mathcal{F}\mathcal{F}_{s}^{*})\varphi+\frac{2}{\sqrt{2}}i(\mathcal{F}^{*})^{2}\cosh\varphi\mathcal{F}$$

$$-\frac{2}{\sqrt{2}}i\mathcal{F}^{2}\mathcal{F}^{*}\cosh\varphi)(\frac{i\mathcal{F}}{\sqrt{2}}\cosh\varphi-i\varphi\sigma-\frac{i\mathcal{F}^{*}}{\sqrt{2}}\cosh\varphi).$$

⋈ *Schrödinger antiferromagnetic thermocomplex solid magnetic $\mathcal{NLS}$ pressure of $\phi(\chi_1)$ tension antiferromagnetic wave energy is*

$$\Upsilon_{afr}^{nls}\phi(\chi_1)=\varkappa\int_{\Phi}((i(\mathcal{F}^{*}\mathcal{F}_{s}-\mathcal{F}\mathcal{F}_{s}^{*})\varphi+\frac{2}{\sqrt{2}}i(\mathcal{F}^{*})^{2}\cosh\varphi\mathcal{F}-\frac{2}{\sqrt{2}}i\mathcal{F}^{2}\mathcal{F}^{*}\cosh\varphi)(\frac{i\mathcal{F}}{\sqrt{2}}\cosh\varphi$$

$$-i\varphi\sigma-\frac{i\mathcal{F}^{*}}{\sqrt{2}}\cosh\varphi)-(i\cosh\varphi(\mathcal{F}^{*}\mathcal{F}_{s}-\mathcal{F}\mathcal{F}_{s}^{*})\mathcal{L}^{*}-\frac{2}{\sqrt{2}}i\mathcal{F}^{2}\mathcal{F}^{*}(\varphi\mathcal{L}^{*}+i\mathcal{L})$$

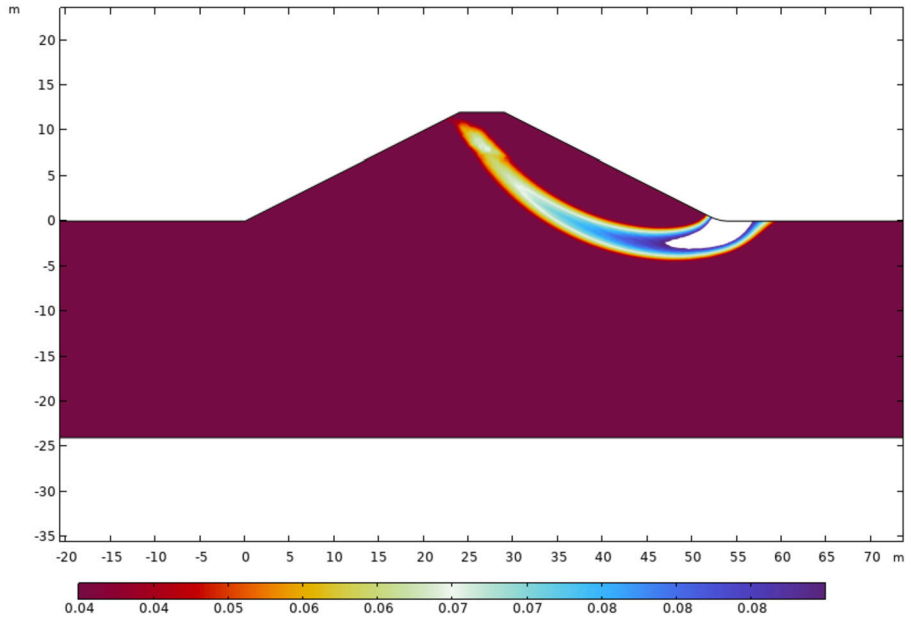

Fig. 1. Dispersive complex $\mathcal{NLS}$ Heisenberg shock optimistic waves for $\phi(\chi_1)$ dam-break intensity

$$+\frac{2}{\sqrt{2}}i(\mathcal{F}^*)^2(\varphi\mathcal{L}^*-i\mathcal{L})\mathcal{F})(-i\sigma\cosh\varphi\mathcal{L}^*+\frac{i\mathcal{F}}{\sqrt{2}}(\varphi\mathcal{L}^*+i\mathcal{L})-\frac{i\mathcal{F}^*}{\sqrt{2}}(\varphi\mathcal{L}^*-i\mathcal{L}))$$
$$+(-\frac{2}{\sqrt{2}}i\mathcal{F}^2\mathcal{F}^*(\varphi\mathcal{L}+i\mathcal{L}^*)+i\cosh\varphi(\mathcal{F}^*\mathcal{F}_s-\mathcal{F}\mathcal{F}_s^*)\mathcal{L}+\frac{2}{\sqrt{2}}i(\mathcal{F}^*)^2\mathcal{F}(\varphi\mathcal{L}$$
$$-i\mathcal{L}^*))(\frac{i\mathcal{F}}{\sqrt{2}}(\varphi\mathcal{L}+i\mathcal{L}^*)-\frac{i\mathcal{F}^*}{\sqrt{2}}(\varphi\mathcal{L}-i\mathcal{L}^*)-i\cosh\varphi\sigma\mathcal{L}))d\Phi,$$

where $\varkappa$ is Heisenberg complex dam-break potential in shallow water (Fig. 1).

4. Heisenberg super-fluid complex magnetic $\phi(\chi_2)$ dam-break antiferromagnetic microfluidics

⋈ *Heisenberg super-fluid complex dispersive $\mathcal{NLS}$ shock electromotive wave for $\phi(\chi_2)$ tension dam-break microfluidics is*

$$\Delta^{nls}\phi(\chi_2)=-\frac{d}{dv}\int_{\Phi}(-(\cosh\varphi(\mathcal{F}_v^*-i\sigma\mathcal{F}_s)\mathcal{L}^*-\frac{1}{\sqrt{2}}i(\mathcal{F}_s^*)^2(\varphi\mathcal{L}^*-i\mathcal{L})$$
$$+\frac{1}{\sqrt{2}}(\varphi\mathcal{L}^*+i\mathcal{L})(i\mathcal{F}_s\mathcal{F}^*+\sigma_v+i\mathcal{F}\sigma\mathcal{F}^*))(-i\sigma\cosh\varphi\mathcal{L}^*+\frac{i\mathcal{F}}{\sqrt{2}}(\varphi\mathcal{L}^*+i\mathcal{L})$$
$$-\frac{i\mathcal{F}^*}{\sqrt{2}}(\varphi\mathcal{L}^*-i\mathcal{L}))+(\varphi(\mathcal{F}_v^*-i\sigma\mathcal{F}_s)+\frac{1}{\sqrt{2}}\cosh\varphi(i\mathcal{F}_s\mathcal{F}^*+\sigma_v+i\mathcal{F}\sigma\mathcal{F}^*)$$
$$-\frac{1}{\sqrt{2}}i(\mathcal{F}_s^*)^2\cosh\varphi)(\frac{i\mathcal{F}}{\sqrt{2}}\cosh\varphi-i\varphi\sigma-\frac{i\mathcal{F}^*}{\sqrt{2}}\cosh\varphi)+(-\frac{1}{\sqrt{2}}i(\mathcal{F}_s^*)^2(\varphi\mathcal{L}-i\mathcal{L}^*)$$
$$+\cosh\varphi\mathcal{L}(\mathcal{F}_v^*-i\sigma\mathcal{F}_s)+\frac{1}{\sqrt{2}}(i\mathcal{F}_s\mathcal{F}^*+\sigma_v+i\mathcal{F}\sigma\mathcal{F}^*)(\varphi\mathcal{L}$$
$$+i\mathcal{L}^*))(\frac{i\mathcal{F}}{\sqrt{2}}(\varphi\mathcal{L}+i\mathcal{L}^*)-\frac{i\mathcal{F}^*}{\sqrt{2}}(\varphi\mathcal{L}-i\mathcal{L}^*)-i\cosh\varphi\sigma\mathcal{L}))d\Phi.$$

Since, it is easy to see that

$$\nabla_v\phi(\chi_2)=(\varphi(\mathcal{F}_v^*-i\sigma\mathcal{F}_s)+\frac{1}{\sqrt{2}}\cosh\varphi(i\mathcal{F}_s\mathcal{F}^*+\sigma_v+i\mathcal{F}\sigma\mathcal{F}^*)-\frac{1}{\sqrt{2}}i(\mathcal{F}_s^*)^2\cosh\varphi)\mathbf{e}_1$$
$$+(-\frac{1}{\sqrt{2}}i(\mathcal{F}_s^*)^2(\varphi\mathcal{L}-i\mathcal{L}^*)+\cosh\varphi\mathcal{L}(\mathcal{F}_v^*-i\sigma\mathcal{F}_s)+\frac{1}{\sqrt{2}}(i\mathcal{F}_s\mathcal{F}^*+\sigma_v+i\mathcal{F}\sigma\mathcal{F}^*)(\varphi\mathcal{L}+i\mathcal{L}^*))\mathbf{e}_2$$
$$+(\cosh\varphi(\mathcal{F}_v^*-i\sigma\mathcal{F}_s)\mathcal{L}^*-\frac{1}{\sqrt{2}}i(\mathcal{F}_s^*)^2(\varphi\mathcal{L}^*-i\mathcal{L})+\frac{1}{\sqrt{2}}(\varphi\mathcal{L}^*+i\mathcal{L})(i\mathcal{F}_s\mathcal{F}^*+\sigma_v+i\mathcal{F}\sigma\mathcal{F}^*))\mathbf{e}_3$$

⋈ *Lorentzian dispersive complex $\mathcal{NLS}$ Heisenberg shock optimistic waves for $\phi(\chi_2)$ dam-break intensity is*

$$\mathcal{F}^{nls}\phi(\chi_2)=(\varphi(\mathcal{F}_v^*-i\sigma\mathcal{F}_s)+\frac{1}{\sqrt{2}}\cosh\varphi(i\mathcal{F}_s\mathcal{F}^*+\sigma_v+i\mathcal{F}\sigma\mathcal{F}^*)-\frac{1}{\sqrt{2}}i(\mathcal{F}_s^*)^2\cosh\varphi)(\frac{i\mathcal{F}}{\sqrt{2}}\cosh\varphi$$

$$-i\varphi\sigma-\frac{i\mathcal{F}^*}{\sqrt{2}}\cosh\varphi)+(-\frac{1}{\sqrt{2}}i(\mathcal{F}_s^*)^2(\varphi\mathcal{L}-i\mathcal{L}^*)+\cosh\varphi\mathcal{L}(\mathcal{F}_\nu^*-i\sigma\mathcal{F}_s)+\frac{1}{\sqrt{2}}(i\mathcal{F}_s\mathcal{F}^*$$
$$+\sigma_\nu+i\mathcal{F}\sigma\mathcal{F}^*)(\varphi\mathcal{L}+i\mathcal{L}^*))(\frac{i\mathcal{F}}{\sqrt{2}}(\varphi\mathcal{L}+i\mathcal{L}^*)-\frac{i\mathcal{F}^*}{\sqrt{2}}(\varphi\mathcal{L}-i\mathcal{L}^*)-i\cosh\varphi\sigma\mathcal{L})$$
$$-(\cosh\varphi(\mathcal{F}_\nu^*-i\sigma\mathcal{F}_s)\mathcal{L}^*-\frac{1}{\sqrt{2}}i(\mathcal{F}_s^*)^2(\varphi\mathcal{L}^*-i\mathcal{L})+\frac{1}{\sqrt{2}}(\varphi\mathcal{L}^*+i\mathcal{L})(i\mathcal{F}_s\mathcal{F}^*$$
$$+\sigma_\nu+i\mathcal{F}\sigma\mathcal{F}^*))(-i\sigma\cosh\varphi\mathcal{L}^*+\frac{i\mathcal{F}}{\sqrt{2}}(\varphi\mathcal{L}^*+i\mathcal{L})-\frac{i\mathcal{F}^*}{\sqrt{2}}(\varphi\mathcal{L}^*-i\mathcal{L})).$$

⋈ *Schrödinger thermocomplex solid magnetic $\mathcal{NLS}$ pressure of $\phi(\chi_2)$ tension wave energy is*

$$\Upsilon^{nls}\phi(\chi_2)=\varkappa\int_\Phi((-\frac{1}{\sqrt{2}}i(\mathcal{F}_s^*)^2(\varphi\mathcal{L}-i\mathcal{L}^*)+\cosh\varphi\mathcal{L}(\mathcal{F}_\nu^*-i\sigma\mathcal{F}_s)+\frac{1}{\sqrt{2}}(i\mathcal{F}_s\mathcal{F}^*+\sigma_\nu$$
$$+i\mathcal{F}\sigma\mathcal{F}^*)(\varphi\mathcal{L}+i\mathcal{L}^*))(\frac{i\mathcal{F}}{\sqrt{2}}(\varphi\mathcal{L}+i\mathcal{L}^*)-\frac{i\mathcal{F}^*}{\sqrt{2}}(\varphi\mathcal{L}-i\mathcal{L}^*)-i\cosh\varphi\sigma\mathcal{L})$$
$$+(\varphi(\mathcal{F}_\nu^*-i\sigma\mathcal{F}_s)+\frac{1}{\sqrt{2}}\cosh\varphi(i\mathcal{F}_s\mathcal{F}^*+\sigma_\nu+i\mathcal{F}\sigma\mathcal{F}^*)-\frac{1}{\sqrt{2}}i(\mathcal{F}_s^*)^2\cosh\varphi)(\frac{i\mathcal{F}}{\sqrt{2}}\cosh\varphi-i\varphi\sigma$$
$$-\frac{i\mathcal{F}^*}{\sqrt{2}}\cosh\varphi)-(\cosh\varphi(\mathcal{F}_\nu^*-i\sigma\mathcal{F}_s)\mathcal{L}^*-\frac{1}{\sqrt{2}}i(\mathcal{F}_s^*)^2(\varphi\mathcal{L}^*-i\mathcal{L})+\frac{1}{\sqrt{2}}(\varphi\mathcal{L}^*$$
$$+i\mathcal{L})(i\mathcal{F}_s\mathcal{F}^*+\sigma_\nu+i\mathcal{F}\sigma\mathcal{F}^*))(-i\sigma\cosh\varphi\mathcal{L}^*+\frac{i\mathcal{F}}{\sqrt{2}}(\varphi\mathcal{L}^*+i\mathcal{L})-\frac{i\mathcal{F}^*}{\sqrt{2}}(\varphi\mathcal{L}^*-i\mathcal{L})))d\Phi,$$

where $\varkappa$ is Heisenberg complex dam-break potential in shallow water.

Some calculations, we get

$$\phi(\chi_2)\times\nabla_s\phi(\chi_2)=(\frac{1}{\sqrt{2}}\cosh\varphi i(\mathcal{F}^*(\sigma_s+\mathcal{F}^*\mathcal{F})+\sigma(\mathcal{F}_s^*+\sigma\mathcal{F}^*))-i\sigma(\mathcal{F}^*)^2\varphi$$
$$-\frac{1}{\sqrt{2}}i(\mathcal{F}^*)^3\cosh\varphi)\mathbf{e}_1+(-i\sigma(\mathcal{F}^*)^2\cosh\varphi\mathcal{L}-\frac{1}{\sqrt{2}}i(\mathcal{F}^*)^3(\varphi\mathcal{L}-i\mathcal{L}^*)+\frac{1}{\sqrt{2}}i(\mathcal{F}^*(\sigma_s$$
$$+\mathcal{F}^*\mathcal{F})+\sigma(\mathcal{F}_s^*+\sigma\mathcal{F}^*))(\varphi\mathcal{L}+i\mathcal{L}^*))\mathbf{e}_2+(\frac{1}{\sqrt{2}}(\varphi\mathcal{L}^*+i\mathcal{L})i(\mathcal{F}^*(\sigma_s$$
$$+\mathcal{F}^*\mathcal{F})+\sigma(\mathcal{F}_s^*+\sigma\mathcal{F}^*))-\frac{1}{\sqrt{2}}i(\mathcal{F}^*)^3(\varphi\mathcal{L}^*-i\mathcal{L})-i\sigma(\mathcal{F}^*)^2\cosh\varphi\mathcal{L}^*)\mathbf{e}_3$$

⋈ *Antiferromagnetic Heisenberg super-fluid complex dispersive $\mathcal{NLS}$ shock electromotive wave for $\phi(\chi_2)$ tension dam-break antiferromagnetic microfluidics is*

$$\Delta_{afr}^{nls}\phi(\chi_2)=-\frac{d}{d\upsilon}\int_\Phi((\frac{i\mathcal{F}}{\sqrt{2}}(\varphi\mathcal{L}+i\mathcal{L}^*)-\frac{i\mathcal{F}^*}{\sqrt{2}}(\varphi\mathcal{L}-i\mathcal{L}^*)-i\cosh\varphi\sigma\mathcal{L})(-i\sigma(\mathcal{F}^*)^2\cosh\varphi\mathcal{L}$$
$$-\frac{1}{\sqrt{2}}i(\mathcal{F}^*)^3(\varphi\mathcal{L}-i\mathcal{L}^*)+\frac{1}{\sqrt{2}}i(\mathcal{F}^*(\sigma_s+\mathcal{F}^*\mathcal{F})+\sigma(\mathcal{F}_s^*+\sigma\mathcal{F}^*))(\varphi\mathcal{L}+i\mathcal{L}^*))$$
$$+(\frac{i\mathcal{F}}{\sqrt{2}}\cosh\varphi-i\varphi\sigma-\frac{i\mathcal{F}^*}{\sqrt{2}}\cosh\varphi)(\frac{1}{\sqrt{2}}\cosh\varphi i(\mathcal{F}^*(\sigma_s+\mathcal{F}^*\mathcal{F})+\sigma(\mathcal{F}_s^*+\sigma\mathcal{F}^*))-i\sigma(\mathcal{F}^*)^2\varphi$$
$$-\frac{1}{\sqrt{2}}i(\mathcal{F}^*)^3\cosh\varphi)-(-i\sigma\cosh\varphi\mathcal{L}^*+\frac{i\mathcal{F}}{\sqrt{2}}(\varphi\mathcal{L}^*+i\mathcal{L})-\frac{i\mathcal{F}^*}{\sqrt{2}}(\varphi\mathcal{L}^*-i\mathcal{L}))(\frac{1}{\sqrt{2}}(\varphi\mathcal{L}^*$$
$$+i\mathcal{L})i(\mathcal{F}^*(\sigma_s+\mathcal{F}^*\mathcal{F})+\sigma(\mathcal{F}_s^*+\sigma\mathcal{F}^*))-\frac{1}{\sqrt{2}}i(\mathcal{F}^*)^3(\varphi\mathcal{L}^*-i\mathcal{L})-i\sigma(\mathcal{F}^*)^2\cosh\varphi\mathcal{L}^*))d\Phi.$$

⋈ *Lorentzian antiferromagnetic dispersive complex $\mathcal{NLS}$ Heisenberg shock optimistic waves for $\phi(\chi_2)$ dam-break antiferromagnetic intensity is*

$$\mathcal{F}_{afr}^{nls}\phi(\chi_2)=(\frac{i\mathcal{F}}{\sqrt{2}}\cosh\varphi-i\varphi\sigma-\frac{i\mathcal{F}^*}{\sqrt{2}}\cosh\varphi)(\frac{1}{\sqrt{2}}\cosh\varphi i(\mathcal{F}^*(\sigma_s+\mathcal{F}^*\mathcal{F})+\sigma(\mathcal{F}_s^*+\sigma\mathcal{F}^*))$$
$$-i\sigma(\mathcal{F}^*)^2\varphi-\frac{1}{\sqrt{2}}i(\mathcal{F}^*)^3\cosh\varphi)+(\frac{i\mathcal{F}}{\sqrt{2}}(\varphi\mathcal{L}+i\mathcal{L}^*)-\frac{i\mathcal{F}^*}{\sqrt{2}}(\varphi\mathcal{L}-i\mathcal{L}^*)$$
$$-i\cosh\varphi\sigma\mathcal{L})(-i\sigma(\mathcal{F}^*)^2\cosh\varphi\mathcal{L}-\frac{1}{\sqrt{2}}i(\mathcal{F}^*)^3(\varphi\mathcal{L}-i\mathcal{L}^*)+\frac{1}{\sqrt{2}}i(\mathcal{F}^*(\sigma_s+\mathcal{F}^*\mathcal{F})$$
$$+\sigma(\mathcal{F}_s^*+\sigma\mathcal{F}^*))(\varphi\mathcal{L}+i\mathcal{L}^*))-(-i\sigma\cosh\varphi\mathcal{L}^*+\frac{i\mathcal{F}}{\sqrt{2}}(\varphi\mathcal{L}^*+i\mathcal{L})$$
$$-\frac{i\mathcal{F}^*}{\sqrt{2}}(\varphi\mathcal{L}^*-i\mathcal{L}))(\frac{1}{\sqrt{2}}(\varphi\mathcal{L}^*+i\mathcal{L})i(\mathcal{F}^*(\sigma_s+\mathcal{F}^*\mathcal{F})+\sigma(\mathcal{F}_s^*+\sigma\mathcal{F}^*))$$

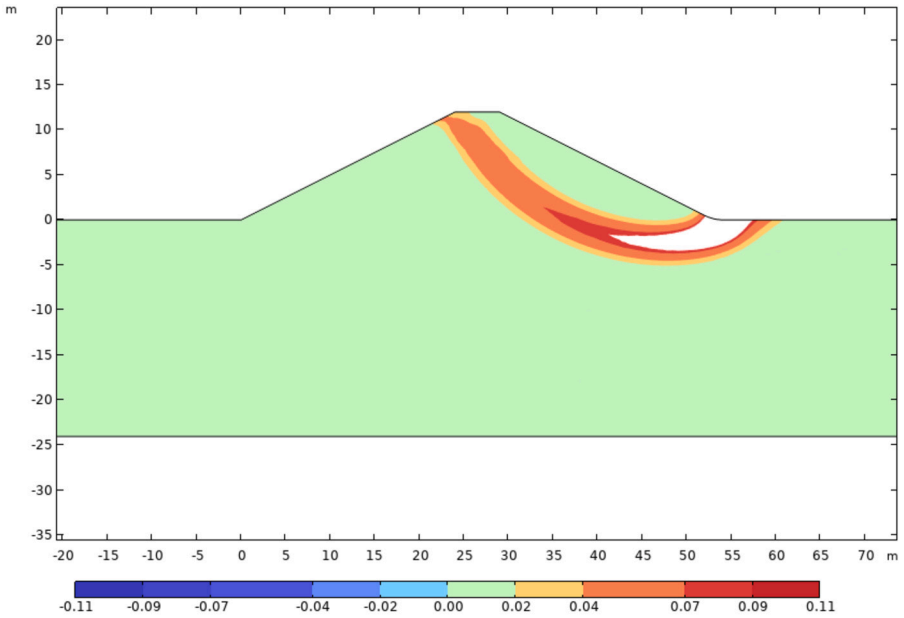

Fig. 2. Dispersive complex $\mathcal{NLS}$ Heisenberg shock optimistic waves for $\phi(\chi_2)$ dam-break intensity

$$-\frac{1}{\sqrt{2}}i(\mathcal{F}^*)^3(\varphi\mathcal{L}^*-i\mathcal{L})-i\sigma(\mathcal{F}^*)^2\cosh\varphi\mathcal{L}^*).$$

⋈ *Schrödinger antiferromagnetic thermocomplex solid magnetic* $\mathcal{NLS}$ *pressure of* $\phi(\chi_2)$ *tension antiferromagnetic wave energy is*

$$\Upsilon^{nls}_{afr}\phi(\chi_2)=\varkappa\int_{\Phi}(-(-i\sigma\cosh\varphi\mathcal{L}^*+\frac{i\mathcal{F}}{\sqrt{2}}(\varphi\mathcal{L}^*+i\mathcal{L})-\frac{i\mathcal{F}^*}{\sqrt{2}}(\varphi\mathcal{L}^*-i\mathcal{L}))(\frac{1}{\sqrt{2}}(\varphi\mathcal{L}^*$$
$$+i\mathcal{L})i(\mathcal{F}^*(\sigma_s+\mathcal{F}^*\mathcal{F})+\sigma(\mathcal{F}_s^*+\sigma\mathcal{F}^*))-\frac{1}{\sqrt{2}}i(\mathcal{F}^*)^3(\varphi\mathcal{L}^*-i\mathcal{L})-i\sigma(\mathcal{F}^*)^2\cosh\varphi\mathcal{L}^*)$$
$$+(\frac{i\mathcal{F}}{\sqrt{2}}\cosh\varphi-i\varphi\sigma-\frac{i\mathcal{F}^*}{\sqrt{2}}\cosh\varphi)(\frac{1}{\sqrt{2}}\cosh\varphi i(\mathcal{F}^*(\sigma_s+\mathcal{F}^*\mathcal{F})+\sigma(\mathcal{F}_s^*+\sigma\mathcal{F}^*))-i\sigma(\mathcal{F}^*)^2\varphi$$
$$-\frac{1}{\sqrt{2}}i(\mathcal{F}^*)^3\cosh\varphi)+(\frac{i\mathcal{F}}{\sqrt{2}}(\varphi\mathcal{L}+i\mathcal{L}^*)-\frac{i\mathcal{F}^*}{\sqrt{2}}(\varphi\mathcal{L}-i\mathcal{L}^*)-i\cosh\varphi\sigma\mathcal{L})(-i\sigma(\mathcal{F}^*)^2\cosh\varphi\mathcal{L}$$
$$-\frac{1}{\sqrt{2}}i(\mathcal{F}^*)^3(\varphi\mathcal{L}-i\mathcal{L}^*)+\frac{1}{\sqrt{2}}i(\mathcal{F}^*(\sigma_s+\mathcal{F}^*\mathcal{F})+\sigma(\mathcal{F}_s^*+\sigma\mathcal{F}^*))(\varphi\mathcal{L}+i\mathcal{L}^*)))d\Phi,$$

where $\varkappa$ *is Heisenberg complex dam-break potential in shallow water (Fig. 2).*

5. Heisenberg super-fluid complex magnetic $\phi(\chi_3)$ dam-break antiferromagnetic microfluidics

⋈ *Heisenberg super-fluid complex dispersive* $\mathcal{NLS}$ *shock electromotive wave for* $\phi(\chi_3)$ *tension dam-break microfluidics is*

$$\Delta^{nls}\phi(\chi_3)=-\frac{d}{dv}\int_{\Phi}((\frac{i\mathcal{F}}{\sqrt{2}}\cosh\varphi-i\varphi\sigma-\frac{i\mathcal{F}^*}{\sqrt{2}}\cosh\varphi)(\varphi(\mathcal{F}_v-i\sigma\mathcal{F}_s)+\frac{1}{\sqrt{2}}i\mathcal{F}\mathcal{F}_s\cosh\varphi$$
$$+\frac{1}{\sqrt{2}}(i\sigma\mathcal{F}\mathcal{F}^*-i\mathcal{F}\mathcal{F}_s^*-\sigma_v)\cosh\varphi)-(-i\sigma\cosh\varphi\mathcal{L}^*+\frac{i\mathcal{F}}{\sqrt{2}}(\varphi\mathcal{L}^*+i\mathcal{L})-\frac{i\mathcal{F}^*}{\sqrt{2}}(\varphi\mathcal{L}^*$$
$$-i\mathcal{L}))(\cosh\varphi\mathcal{L}^*(\mathcal{F}_v-i\sigma\mathcal{F}_s)+\frac{1}{\sqrt{2}}(i\sigma\mathcal{F}\mathcal{F}^*-i\mathcal{F}\mathcal{F}_s^*-\sigma_v)(\varphi\mathcal{L}^*-i\mathcal{L})$$
$$+\frac{1}{\sqrt{2}}i\mathcal{F}\mathcal{F}_s(\varphi\mathcal{L}^*+i\mathcal{L}))+(\frac{i\mathcal{F}}{\sqrt{2}}(\varphi\mathcal{L}+i\mathcal{L}^*)-\frac{i\mathcal{F}^*}{\sqrt{2}}(\varphi\mathcal{L}-i\mathcal{L}^*)-i\cosh\varphi\sigma\mathcal{L})(\frac{1}{\sqrt{2}}(\varphi\mathcal{L}$$
$$-i\mathcal{L}^*)(i\sigma\mathcal{F}\mathcal{F}^*-i\mathcal{F}\mathcal{F}_s^*-\sigma_v)+\frac{1}{\sqrt{2}}i(\varphi\mathcal{L}+i\mathcal{L}^*)\mathcal{F}\mathcal{F}_s+\cosh\varphi\mathcal{L}(\mathcal{F}_v-i\sigma\mathcal{F}_s)))d\Phi.$$

On the other hand, we get

$$\nabla_v\phi(\chi_3)=(\varphi(\mathcal{F}_v-i\sigma\mathcal{F}_s)+\frac{1}{\sqrt{2}}i\mathcal{F}\mathcal{F}_s\cosh\varphi+\frac{1}{\sqrt{2}}(i\sigma\mathcal{F}\mathcal{F}^*-i\mathcal{F}\mathcal{F}_s^*-\sigma_v)\cosh\varphi)\mathbf{e}_1$$
$$+(\frac{1}{\sqrt{2}}(\varphi\mathcal{L}-i\mathcal{L}^*)(i\sigma\mathcal{F}\mathcal{F}^*-i\mathcal{F}\mathcal{F}_s^*-\sigma_v)+\frac{1}{\sqrt{2}}i(\varphi\mathcal{L}+i\mathcal{L}^*)\mathcal{F}\mathcal{F}_s+\cosh\varphi\mathcal{L}(\mathcal{F}_v-i\sigma\mathcal{F}_s))\mathbf{e}_2$$

$$+(\cosh\varphi\mathcal{L}^*(\mathcal{F}_\nu - i\sigma\mathcal{F}_s) + \frac{1}{\sqrt{2}}(i\sigma\mathcal{F}\mathcal{F}^* - i\mathcal{F}\mathcal{F}_s^* - \sigma_\nu)(\varphi\mathcal{L}^* - i\mathcal{L}) + \frac{1}{\sqrt{2}}i\mathcal{F}\mathcal{F}_s(\varphi\mathcal{L}^* + i\mathcal{L}))\mathbf{e}_3.$$

⋈ *Lorentzian dispersive complex $\mathcal{NLS}$ Heisenberg shock optimistic waves for $\phi(\chi_3)$ dam-break intensity is*

$$\mathcal{F}^{nls}\phi(\chi_3) = (\frac{i\mathcal{F}}{\sqrt{2}}\cosh\varphi - i\varphi\sigma - \frac{i\mathcal{F}^*}{\sqrt{2}}\cosh\varphi)(\varphi(\mathcal{F}_\nu - i\sigma\mathcal{F}_s) + \frac{1}{\sqrt{2}}i\mathcal{F}\mathcal{F}_s\cosh\varphi$$
$$+\frac{1}{\sqrt{2}}(i\sigma\mathcal{F}\mathcal{F}^* - i\mathcal{F}\mathcal{F}_s^* - \sigma_\nu)\cosh\varphi) + (\frac{i\mathcal{F}}{\sqrt{2}}(\varphi\mathcal{L} + i\mathcal{L}^*) - \frac{i\mathcal{F}^*}{\sqrt{2}}(\varphi\mathcal{L} - i\mathcal{L}^*)$$
$$-i\cosh\varphi\sigma\mathcal{L})(\frac{1}{\sqrt{2}}(\varphi\mathcal{L} - i\mathcal{L}^*)(i\sigma\mathcal{F}\mathcal{F}^* - i\mathcal{F}\mathcal{F}_s^* - \sigma_\nu) + \frac{1}{\sqrt{2}}i(\varphi\mathcal{L} + i\mathcal{L}^*)\mathcal{F}\mathcal{F}_s$$
$$+\cosh\varphi\mathcal{L}(\mathcal{F}_\nu - i\sigma\mathcal{F}_s)) - (-i\sigma\cosh\varphi\mathcal{L}^* + \frac{i\mathcal{F}}{\sqrt{2}}(\varphi\mathcal{L}^* + i\mathcal{L}) - \frac{i\mathcal{F}^*}{\sqrt{2}}(\varphi\mathcal{L}^*$$
$$-i\mathcal{L}))(\cosh\varphi\mathcal{L}^*(\mathcal{F}_\nu - i\sigma\mathcal{F}_s) + \frac{1}{\sqrt{2}}(i\sigma\mathcal{F}\mathcal{F}^* - i\mathcal{F}\mathcal{F}_s^*$$
$$-\sigma_\nu)(\varphi\mathcal{L}^* - i\mathcal{L}) + \frac{1}{\sqrt{2}}i\mathcal{F}\mathcal{F}_s(\varphi\mathcal{L}^* + i\mathcal{L}))$$

⋈ *Schrödinger thermocomplex solid magnetic $\mathcal{NLS}$ pressure of $\phi(\chi_3)$ tension wave energy is*

$$\Upsilon^{nls}\phi(\chi_3) = \varkappa\int_\Phi((\frac{i\mathcal{F}}{\sqrt{2}}(\varphi\mathcal{L} + i\mathcal{L}^*) - \frac{i\mathcal{F}^*}{\sqrt{2}}(\varphi\mathcal{L} - i\mathcal{L}^*) - i\cosh\varphi\sigma\mathcal{L})(\frac{1}{\sqrt{2}}(\varphi\mathcal{L}$$
$$-i\mathcal{L}^*)(i\sigma\mathcal{F}\mathcal{F}^* - i\mathcal{F}\mathcal{F}_s^* - \sigma_\nu) + \frac{1}{\sqrt{2}}i(\varphi\mathcal{L} + i\mathcal{L}^*)\mathcal{F}\mathcal{F}_s + \cosh\varphi\mathcal{L}(\mathcal{F}_\nu - i\sigma\mathcal{F}_s))$$
$$+(\frac{i\mathcal{F}}{\sqrt{2}}\cosh\varphi - i\varphi\sigma - \frac{i\mathcal{F}^*}{\sqrt{2}}\cosh\varphi)(\varphi(\mathcal{F}_\nu - i\sigma\mathcal{F}_s) + \frac{1}{\sqrt{2}}i\mathcal{F}\mathcal{F}_s\cosh\varphi + \frac{1}{\sqrt{2}}(i\sigma\mathcal{F}\mathcal{F}^*$$
$$-i\mathcal{F}\mathcal{F}_s^* - \sigma_\nu)\cosh\varphi) - (-i\sigma\cosh\varphi\mathcal{L}^* + \frac{i\mathcal{F}}{\sqrt{2}}(\varphi\mathcal{L}^* + i\mathcal{L}) - \frac{i\mathcal{F}^*}{\sqrt{2}}(\varphi\mathcal{L}^* - i\mathcal{L}))(\cosh\varphi\mathcal{L}^*(\mathcal{F}_\nu$$
$$-i\sigma\mathcal{F}_s) + \frac{1}{\sqrt{2}}(i\sigma\mathcal{F}\mathcal{F}^* - i\mathcal{F}\mathcal{F}_s^* - \sigma_\nu)(\varphi\mathcal{L}^* - i\mathcal{L}) + \frac{1}{\sqrt{2}}i\mathcal{F}\mathcal{F}_s(\varphi\mathcal{L}^* + i\mathcal{L})))d\Phi,$$

where $\varkappa$ is Heisenberg complex dam-break potential in shallow water.

Since, we obtain

$$\phi(\chi_3)\times\nabla_s\phi(\chi_3) = (i(\mathcal{F})^2\varphi\sigma + \frac{1}{\sqrt{2}}i(\mathcal{F})^3\cosh\varphi + \frac{1}{\sqrt{2}}i(\sigma(\mathcal{F}_s - \sigma\mathcal{F}) - \mathcal{F}(\mathcal{F}^*\mathcal{F} - \sigma_s))\cosh\varphi)\mathbf{e}_1$$
$$+(\frac{1}{\sqrt{2}}i(\sigma(\mathcal{F}_s - \sigma\mathcal{F}) - \mathcal{F}(\mathcal{F}^*\mathcal{F} - \sigma_s))(\varphi\mathcal{L} - i\mathcal{L}^*) + i(\mathcal{F})^2\cosh\varphi\sigma\mathcal{L} + \frac{1}{\sqrt{2}}i(\mathcal{F})^3(\varphi\mathcal{L} + i\mathcal{L}^*))\mathbf{e}_2$$
$$+(\frac{1}{\sqrt{2}}i(\sigma(\mathcal{F}_s - \sigma\mathcal{F}) - \mathcal{F}(\mathcal{F}^*\mathcal{F} - \sigma_s))(\varphi\mathcal{L}^* - i\mathcal{L}) + i(\mathcal{F})^2\cosh\varphi\mathcal{L}^*\sigma + \frac{1}{\sqrt{2}}i(\mathcal{F})^3(\varphi\mathcal{L}^* + i\mathcal{L}))\mathbf{e}_3.$$

⋈ *Antiferromagnetic Heisenberg super-fluid complex dispersive $\mathcal{NLS}$ shock electromotive wave for $\phi(\chi_3)$ tension dam-break antiferromagnetic microfluidics is*

$$\Delta_{afr}^{nls}\phi(\chi_3) = -\frac{d}{d\upsilon}\int_\Phi((\frac{1}{\sqrt{2}}i(\sigma(\mathcal{F}_s - \sigma\mathcal{F}) - \mathcal{F}(\mathcal{F}^*\mathcal{F} - \sigma_s))(\varphi\mathcal{L} - i\mathcal{L}^*)$$
$$+i(\mathcal{F})^2\cosh\varphi\sigma\mathcal{L} + \frac{1}{\sqrt{2}}i(\mathcal{F})^3(\varphi\mathcal{L} + i\mathcal{L}^*))(\frac{i\mathcal{F}}{\sqrt{2}}(\varphi\mathcal{L} + i\mathcal{L}^*)$$
$$-\frac{i\mathcal{F}^*}{\sqrt{2}}(\varphi\mathcal{L} - i\mathcal{L}^*) - i\cosh\varphi\sigma\mathcal{L}) - (-i\sigma\cosh\varphi\mathcal{L}^* + \frac{i\mathcal{F}}{\sqrt{2}}(\varphi\mathcal{L}^* + i\mathcal{L})$$
$$-\frac{i\mathcal{F}^*}{\sqrt{2}}(\varphi\mathcal{L}^* - i\mathcal{L}))(\frac{1}{\sqrt{2}}i(\sigma(\mathcal{F}_s - \sigma\mathcal{F}) - \mathcal{F}(\mathcal{F}^*\mathcal{F}$$
$$-\sigma_s))(\varphi\mathcal{L}^* - i\mathcal{L}) + i(\mathcal{F})^2\cosh\varphi\mathcal{L}^*\sigma + \frac{1}{\sqrt{2}}i(\mathcal{F})^3(\varphi\mathcal{L}^* + i\mathcal{L}))$$
$$+(i(\mathcal{F})^2\varphi\sigma + \frac{1}{\sqrt{2}}i(\mathcal{F})^3\cosh\varphi + \frac{1}{\sqrt{2}}i(\sigma(\mathcal{F}_s - \sigma\mathcal{F})$$
$$-\mathcal{F}(\mathcal{F}^*\mathcal{F} - \sigma_s))\cosh\varphi)(\frac{i\mathcal{F}}{\sqrt{2}}\cosh\varphi - i\varphi\sigma - \frac{i\mathcal{F}^*}{\sqrt{2}}\cosh\varphi))d\Phi.$$

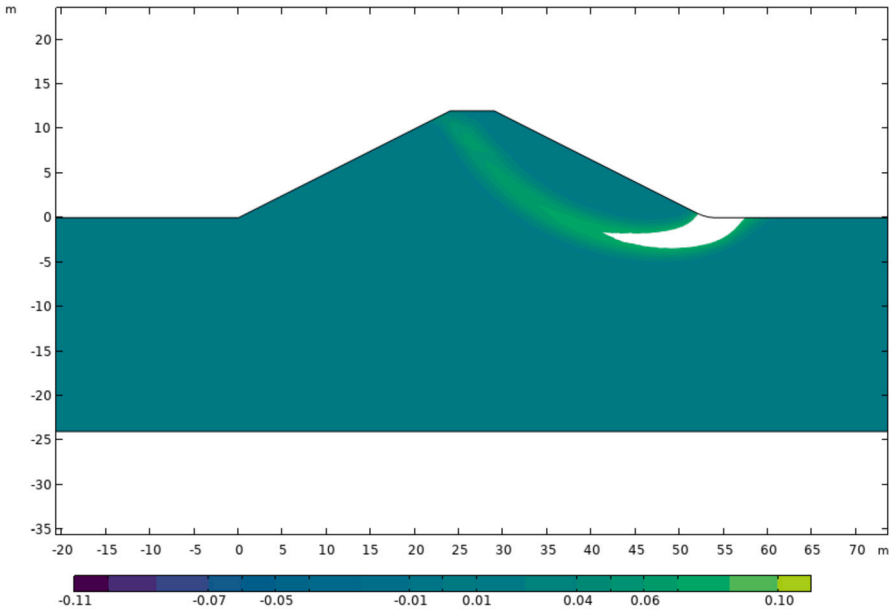

Fig. 3. Dispersive complex $\mathcal{NLS}$ Heisenberg shock optimistic waves for $\phi(\chi_3)$ dam-break intensity.

⋈ *Lorentzian antiferromagnetic dispersive complex $\mathcal{NLS}$ Heisenberg shock optimistic waves for $\phi(\chi_3)$ dam-break antiferromagnetic intensity is*

$$\mathcal{F}_{afr}^{nls}\phi(\chi_3) = -(-i\sigma\cosh\varphi\mathcal{L}^* + \frac{i\mathcal{F}}{\sqrt{2}}(\varphi\mathcal{L}^* + i\mathcal{L}) - \frac{i\mathcal{F}^*}{\sqrt{2}}(\varphi\mathcal{L}^* - i\mathcal{L}))(\frac{1}{\sqrt{2}}i(\sigma(\mathcal{F}_s$$
$$-\sigma\mathcal{F}) - \mathcal{F}(\mathcal{F}^*\mathcal{F} - \sigma_s))(\varphi\mathcal{L}^* - i\mathcal{L}) + i(\mathcal{F})^2\cosh\varphi\mathcal{L}^*\sigma + \frac{1}{\sqrt{2}}i(\mathcal{F})^3(\varphi\mathcal{L}^* + i\mathcal{L}))$$
$$(i(\mathcal{F})^2\varphi\sigma + \frac{1}{\sqrt{2}}i(\mathcal{F})^3\cosh\varphi + \frac{1}{\sqrt{2}}i(\sigma(\mathcal{F}_s - \sigma\mathcal{F}) - \mathcal{F}(\mathcal{F}^*\mathcal{F} - \sigma_s))\cosh\varphi)(\frac{i\mathcal{F}}{\sqrt{2}}\cosh\varphi$$
$$-i\varphi\sigma - \frac{i\mathcal{F}^*}{\sqrt{2}}\cosh\varphi) + (\frac{1}{\sqrt{2}}i(\sigma(\mathcal{F}_s - \sigma\mathcal{F}) - \mathcal{F}(\mathcal{F}^*\mathcal{F} - \sigma_s))(\varphi\mathcal{L} - i\mathcal{L}^*) + i(\mathcal{F})^2\cosh\varphi\sigma\mathcal{L}$$
$$+\frac{1}{\sqrt{2}}i(\mathcal{F})^3(\varphi\mathcal{L} + i\mathcal{L}^*))(\frac{i\mathcal{F}}{\sqrt{2}}(\varphi\mathcal{L} + i\mathcal{L}^*) - \frac{i\mathcal{F}^*}{\sqrt{2}}(\varphi\mathcal{L} - i\mathcal{L}^*) - i\cosh\varphi\sigma\mathcal{L}).$$

⋈ *Schrödinger antiferromagnetic thermocomplex solid magnetic $\mathcal{NLS}$ pressure of $\phi(\chi_3)$ tension antiferromagnetic wave energy is*

$$\Upsilon_{afr}^{nls}\phi(\chi_3) = \varkappa\int_{\Phi}((i(\mathcal{F})^2\varphi\sigma + \frac{1}{\sqrt{2}}i(\mathcal{F})^3\cosh\varphi + \frac{1}{\sqrt{2}}i(\sigma(\mathcal{F}_s - \sigma\mathcal{F}) - \mathcal{F}(\mathcal{F}^*\mathcal{F}$$
$$-\sigma_s))\cosh\varphi)(\frac{i\mathcal{F}}{\sqrt{2}}\cosh\varphi - i\varphi\sigma - \frac{i\mathcal{F}^*}{\sqrt{2}}\cosh\varphi) + (\frac{1}{\sqrt{2}}i(\sigma(\mathcal{F}_s - \sigma\mathcal{F}) - \mathcal{F}(\mathcal{F}^*\mathcal{F} - \sigma_s))(\varphi\mathcal{L}$$
$$-i\mathcal{L}^*) + i(\mathcal{F})^2\cosh\varphi\sigma\mathcal{L} + \frac{1}{\sqrt{2}}i(\mathcal{F})^3(\varphi\mathcal{L} + i\mathcal{L}^*))(\frac{i\mathcal{F}}{\sqrt{2}}(\varphi\mathcal{L} + i\mathcal{L}^*) - \frac{i\mathcal{F}^*}{\sqrt{2}}(\varphi\mathcal{L} - i\mathcal{L}^*)$$
$$-i\cosh\varphi\sigma\mathcal{L}) - (\frac{1}{\sqrt{2}}i(\sigma(\mathcal{F}_s - \sigma\mathcal{F}) - \mathcal{F}(\mathcal{F}^*\mathcal{F} - \sigma_s))(\varphi\mathcal{L}^* - i\mathcal{L}) + i(\mathcal{F})^2\cosh\varphi\mathcal{L}^*\sigma$$
$$+\frac{1}{\sqrt{2}}i(\mathcal{F})^3(\varphi\mathcal{L}^* + i\mathcal{L}))(-i\sigma\cosh\varphi\mathcal{L}^* + \frac{i\mathcal{F}}{\sqrt{2}}(\varphi\mathcal{L}^* + i\mathcal{L}) - \frac{i\mathcal{F}^*}{\sqrt{2}}(\varphi\mathcal{L}^* - i\mathcal{L})))d\Phi,$$

where $\varkappa$ is Heisenberg complex dam-break potential in shallow water (Fig. 3).

6. Conclusion

In this study, we have presented a comprehensive mechanical modeling framework for complex nonlinear Schrödinger (NLS) shock optimistic waves within a Schrödinger-based formulation, incorporating antiferromagnetic Heisenberg superfluid dynamics and Lorentzian hermitian space. Our analysis demonstrates that the interplay between dispersive NLS shock waves and antiferromagnetic microfluidics leads to novel electromotive tension effects, which are critical for understanding wave energy propagation in shallow water environments.

The constructed model successfully captures the dam-break antiferromagnetic intensity in a hermitian space, providing insights into the microscale dynamics of shock waves under nonlinear constraints. Furthermore, the Schrödinger-based antiferromagnetic thermocomplex framework elucidates the relationship between magnetic NLS pressure and wave energy dissipation, offering a robust theoretical foundation for future experimental and computational studies in wave energy conversion.

Future research should explore the application of machine learning and advanced computational fluid dynamics (CFD) techniques to optimize wave energy extraction, as highlighted in A Review on the Progress and Research Directions of Ocean Engineering. Extending the current model to incorporate stochastic wave climate variability and climate change impacts will further enhance its predictive capabilities.

CRediT authorship contribution statement

Fatih Şevgin: Writing – review & editing, Writing – original draft, Visualization, Validation, Resources, Project administration, Methodology, Funding acquisition, Formal analysis, Data curation, Conceptualization. **Talat Körpinar:** Conceptualization, Data curation, Formal analysis, Investigation, Software, Validation, Writing – original draft, Writing – review & editing. **Ali Akgül:** Formal analysis, Methodology, Visualization, Writing – original draft, Writing – review & editing. **Qasem Al-Mdallal:** Funding acquisition, Investigation, Software.

Declaration of competing interest

I am the corresponding author and on behalf of all authors I declare that we have no known competing financial interests or personal relationships that could have appeared to influence the work reported in this paper.

References

[1] Folley M, Whittaker TJT. Analysis of the nearshore wave energy resource. Renew Energy 2009;34(7):1709–15.
[2] Tavakoli S, Khojasteh D, Haghani M, Hirdaris S. A review on the progress and research directions of ocean engineering. Ocean Eng 2023;272:113617.
[3] Chen M, Xiao P, Zhang Z, Sun L, Li F. Effects of the end-stop mechanism on the nonlinear dynamics and power generation of a point absorber in regular waves. Ocean Eng 2021;242:110123.
[4] Aderinto T, Li H. Ocean wave energy converters: status and challenges. Energies 2018;11(5):1250.
[5] Bienaimé T, Isoard M, Fontaine Q, Bramati A, Kamchatnov AM, Glorieux Q, et al. Quantitative analysis of shock wave dynamics in a fluid of light. Phys Rev Lett 2021;126(18):183901.
[6] Wave Energy Harnessing in Shallow Water through Oscillating Bodies; 2023.
[7] Negri M, Malavasi S. Wave energy harnessing in shallow water through oscillating bodies. Energies 2018;11(10):2730.
[8] Marchesi E, Negri M, Malavasi S. Development and analysis of a numerical model for a two-oscillating-body wave energy converter in shallow water. Ocean Eng 2020;214:107765.
[9] Peng J, Huang C, Xue M, Feng R, Zhou E, Zhong Z, et al. Storage regulation mechanism and control strategy of a hydraulic wave power generation system. Energies 2024;17(16):4151.
[10] Taniuti T. Non-linear wave propagation: with applications to physics and magnetohydrodynamics. Academic Press; 1964.
[11] Ebrahimi F, Mohammadi K, Barouti MM, Habibi M. Wave propagation analysis of a spinning porous graphene nanoplatelet-reinforced nanoshell. Waves Random Complex Media 2021;31(6):1655–81.
[12] Jia Y, Zhang S, Wang P, Ji K. A method for detecting surface defects in railhead by magnetic flux leakage. Appl Sci 2021;11(20):9489.
[13] Kamchatnov AM. Dispersive shock wave theory for nonintegrable equations. Phys Rev E 2019;99(1):012203.
[14] Bates PD, Horritt MS, Fewtrell TJ. A simple inertial formulation of the shallow water equations for efficient two-dimensional flood inundation modelling. J Hydrol 2010;387(1–2):33–45.
[15] Praštalo P, Uljarević M, Vukomanović R. Effect of breach parameters and progression curves on dam failure hydrograph. Civ Eng J 2024;10(02).
[16] El-Baradei SA, El-Abd M, Hazem N. Estimate of power output from hydraulic jumps generated downstream from barrages. J Human Earth Future 2024;5(1):72–84.
[17] Djunur LH, Pallu MS, Karamma R, Bakri B. Effect of porous rectangular type baffle block angle on hydraulic jump downstream of spillway. Civ Eng J 2024;10(10):3173–93.
[18] Abbas N, Rehman KU, Shatanawi W, Al-Eid AA. Theoretical study of non-Newtonian micropolar nanofluid flow over an exponentially stretching surface with free stream velocity. Adv Mech Eng 2022;14(7):16878132221107790.
[19] Shatanawi W, Abbas N, Shatnawi TA, Hasan F. Heat and mass transfer of generalized Fourier and Fick's law for second-grade fluid flow at slendering vertical Riga sheet. Heliyon 2023;9(3).
[20] Sevgin F. Machine learning-based temperature forecasting for sustainable climate change adaptation and mitigation. Sustainability 2025;17(5):1812.
[21] Nazir A, Abbas N, Shatanawi W. On stability analysis of a mathematical model of a society confronting with internal extremism. Int J Mod Phys B 2023;37(07):2350065.
[22] Nadeem S, Amin A, Abbas N. On the stagnation point flow of nanomaterial with base viscoelastic micropolar fluid over a stretching surface. Alex Eng J 2020;59(3):1751–60.
[23] Awan AU, Shahzad MH, Nadeem S, Hamam H, Ahammad NA, Arshad A. Investigation of sutterby fluid flow through elliptic multi-stenosed artery: analytical solutions of blood flow problem. Multidiscip Model Mater Struct 2025;21(1):199–216.
[24] Ullah I, Arif M, Nadeem S, Alzabut J. Numerical computations of MHD mixed convection flow of Bingham fluid in a porous square chamber with a wavy cylinder. Int J Thermofluids 2024;24:100938.
[25] Silva D, Rusu E, Guedes Soares C. High-resolution wave energy assessment in shallow water accounting for tides. Energies 2016;9(9):761.
[26] Rusu L. An evaluation of the synergy between the wave and wind energy along the West Iberian nearshore. Energy Convers Manag X 2023;20:100453.
[27] Lucas C, Silva D, Soares CG. Climatic directional wave spectra in coastal sites. Coast Eng 2023;180:104255.
[28] Bhowmick SA, Ratheesh S, Sharma R, Basu S, Kumar R. A simplified assimilation scheme for a coastal wave model using concepts of particle filter. Pure Appl Geophys 2020;177:1167–81.
[29] Nguyen P, Thorstensen A, Sorooshian S, Hsu K, AghaKouchak A, Sanders B, et al. A high resolution coupled hydrologic–hydraulic model (HiResFlood-UCI) for flash flood modeling. J Hydrol 2016;541:401–20.
[30] Huang B, Zhang C, Adamovich I, Akishev Y, Shao T. Surface ionization wave propagation in the nanosecond pulsed surface dielectric barrier discharge: the influence of dielectric material and pulse repetition rate. Plasma Sources Sci Technol 2020;29(4):044001.
[31] Zandi-Baghche-Maryam A, Dini A, Hosseini M. Wave propagation analysis of inhomogeneous multi–nanoplate systems subjected to a thermal field considering surface and flexoelectricity effects. Waves Random Complex Media 2022:1–28.
[32] Körpinar T, Körpinar Z. Antiferromagnetic Schrödinger electromotive microscale in Minkowski space. Opt Quantum Electron 2023;55(8):681.
[33] Ali I, Rizvi STR, Abbas SO, Zhou Q. Optical solitons for modulated compressional dispersive Alfven and Heisenberg ferromagnetic spin chains. Results Phys 2019;15:102714.
[34] Seadawy AR, Arshad M, Lu D. The weakly nonlinear wave propagation theory for the Kelvin-Helmholtz instability in magnetohydrodynamics flows. Chaos Solitons Fractals 2020;139:110141.
[35] Zhang Y, Zang W, Zheng J, Cappietti L, Zhang J, Zheng Y, et al. The influence of waves propagating with the current on the wake of a tidal stream turbine. Appl Energy 2021;290:116729.
[36] Abu-Mulaweh HI. A review of research on laminar mixed convection flow over backward- and forward-facing steps. Int J Therm Sci 2003;42(9):897–909.
[37] Abu-Nada E. Application of nanofluids for heat transfer enhancement of separated flows encountered in a backward facing step. Int J Heat Fluid Flow 2008;29(1):242–9.
[38] Corcione M. Empirical correlating equations for predicting the effective thermal conductivity and dynamic viscosity of nanofluids. Energy Convers Manag 2011;52(1):789–93.
[39] Das SE, Ozisik M, Bayram M, Secer A, Albayrak P. Optical solitons of a cubic-quartic nonlinear Schrödinger equation with parabolic law nonlinearity in optical metamaterials. Int J Geom Methods Mod Phys 2023;20(13):2350235.
[40] Massel SR. Ocean surface waves: their physics and prediction. Vol., vol. 45. World Scientific; 2017.
[41] Shi W, Yan C, Ren Z, Yuan Z, Liu Y, Zheng S, et al. Review on the development of marine floating photovoltaic systems. Ocean Eng 2023;286:115560.
[42] Wiberg PL, Sherwood CR. Calculating wave-generated bottom orbital velocities from surface-wave parameters. Comput Geosci 2008;34(10):1243–62.
[43] Wang X, Bezryadina A, Chen Z, Makris KG, Christodoulides DN, Stegeman GI. Observation of two-dimensional surface solitons. Phys Rev Lett 2007;98(12):123903.
[44] Benetazzo A, Carniel S, Sclavo M, Bergamasco A. Wave–current interaction: effect on the wave field in a semi-enclosed basin. Ocean Model 2013;70:152–65.
[45] Esler JG, Pearce JD. Dispersive dam-break and lock-exchange flows in a two-layer fluid. J Fluid Mech 2011;667:555–85.

[46] Xu W, Liao H, Yang Y, Wu C. Turbulent flow and energy dissipation in plunge pool of high arch dam. J Hydraul Res 2002;40(4):471–6.
[47] Witt A, Stewart K, Hadjerioua B. Predicting total dissolved gas travel time in hydropower reservoirs. J Environ Eng 2017;143(12):06017011.
[48] Kim SJ, Kang BJ, Puc U, Kim WT, Jazbinsek M, Rotermund F, et al. Highly nonlinear optical organic crystals for efficient terahertz wave generation, detection, and applications. Adv Opt Mater 2021;9(23):2101019.
[49] Osman MS, Almusawa H, Tariq KU, Anwar S, Kumar S, Younis M, et al. On global behavior for complex soliton solutions of the perturbed nonlinear Schrödinger equation in nonlinear optical fibers. J Ocean Eng Sci 2022;7(5):431–43.

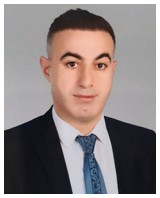

Fatih Şevgin was born in Van in 1982. He was graduated from Dicle University, Faculty of Engineering and Architecture, Department of Civil Engineering. He received his master's degree from Fırat University, Faculty of Engineering, Department of Civil Engineering, Hydraulics and received his PhD from Dicle University Faculty of Engineering, Department of Civil Engineering, Department of Hydraulics, in 2021. He is currently Asst. Prof. at Muş Alparslan University.